JMES The International Journal of
Mechanical Engineering and Sciences
https://iptek.its.ac.id/index.php/jmes
e-ISSN 2580-7471

# Performance of a Savonius Turbine with Circular Cylinders Installed in Front of the Convex Blade and Next to the Concave Blade

Dhia Fairuz Shabrina[1]*, Tri Yogi Yuwono [1]

[1]Department of Mechanical Engineering, ITS, Sukolilo Surabaya 60111, Indonesia

*Received: 4 November 2024, Revised: 13 March 2025, Accepted: 18 March 2025*

**Abstract**

Energy demand is found to be increasing alongside population growth. With fossil energy resources depleting, the necessity for utilizing renewable energy sources, such as wind energy, is recognized. The Savonius wind turbine, characterized by simple construction and the ability to operate at low angular speeds, is noted for its poor efficiency. Circular cylinders were installed to evaluate their impact on turbine performance. Experiments were conducted using two configurations. In the first configuration, a circular cylinder was placed beside the concave blade. In the second configuration, circular cylinders were installed next to the concave blade and in front of the convex blade. Wind speeds were varied at 4, 5, 6, and 7 m/s, respectively. The coefficients of moment, power, and static torque were obtained. Analysis indicated that adding the cylinders in both configurations did not significantly enhance the coefficients of power and moment but did improve the turbine's ability to self-start. For the turbine with the circular cylinder installed, increasing wind speed resulted in decreasing relative performance compared to the conventional turbine.

**Keywords: Circular Cylinder, Coefficient of Moment, Coefficient of Power, Coefficient of Static Torque, Savonius Turbine**

## 1. Introduction

From 2010 to 2020, Indonesia experienced an average population growth rate of 1.25 per cent per year [1]. This growing population has increased energy demand, projected to rise at an average annual rate of 3.5 per cent from 2019 to 2050 [2]. As of 2020, fossil energy sources accounted for 88.8 per cent of the total primary energy supply [2]. However, these non-renewable fossil energy reserves are depleting and will eventually be exhausted. Thus, transitioning to green energy sources is essential to replace fossil energy. Wind energy is a particularly promising option for Indonesia. The country has significant potential for low-speed wind energy, with onshore wind speeds averaging between 3 and 7 m/s [3]. Indonesia's estimated wind energy potential stands at 60,647 MW, yet the installed capacity was only 154 MW by 2020 [2].

One viable technology for harnessing this wind energy is the Savonius wind turbine, which is well-suited for low wind speeds typical in Indonesia. Created by S. J. Savonius, this turbine features blades shaped like half-cylinders, with a cross-section resembling the letter "S." The concave blade faces the wind flow, while the convex blade faces away. The turbine operates by exploiting the difference in drag forces between these blades, generating torque and enabling rotation. The Savonius wind turbine offers several advantages, including simple construction, low cost, and efficient operation at low rotational speeds. It provides high starting torque even at low wind speeds, although its overall efficiency is lower than other wind turbine designs [4].

Numerous studies have focused on enhancing the performance of the Savonius turbine. Researchers, including [5–10], have explored various blade shape modifications to optimize turbine efficiency. Some studies have utilized flat plate deflectors to reduce the drag force on the convex blade and direct airflow toward the concave blade, resulting in improved performance, as demonstrated by [11, 12]. Other investigations have experimented with different deflector designs. For instance, [13] employed a porous deflector, [14] used curved plate deflectors, and [15] introduced an airfoil-shaped deflector. Additionally, [16] innovated by integrating a rotating deflector with the turbine. Notably, a study by [17] combined blade shape modifications with deflector enhancements to achieve even greater performance improvements for the Savonius turbine.

Research by [18, 19] has demonstrated enhancements in the performance of the Savonius turbine by incorporating a circular cylinder positioned in front of the convex blade to reduce drag. This drag reduction occurs due to a decrease in pressure in front of the convex blade. [18] found that a distance ratio of the cylinder

*Corresponding author. Email: dhia@its.ac.id,

to the convex blade (S/D) between 1.4 and 1.8 could increase the turbine's coefficient of power, achieving a maximum increase of 12.2 per cent compared to a conventional turbine at S/D = 1.4. Meanwhile, Sakti and Triyogi [19] reported a maximum coefficient of power increase of 10.2 percent in their experimental studies and 8.8 percent in numerical studies at the same S/D ratio.

In parallel, numerical studies by [20–22] have focused on enhancing the performance of the Savonius turbine by placing a circular cylinder adjacent to the concave blade to boost the drag force on that blade. This increase in drag is attributed to the nozzle effect created between the cylinder and the concave blade. One study by Setiawan et al. demonstrated that a maximum coefficient of power increase of 41.18 percent was achieved by varying the cylinder diameter and stagger angle. In another investigation, varying the cylinder diameter resulted in a maximum power coefficient increase of 28 per cent compared to a conventional turbine. Further numerical studies by Setiawan et al. explored variations in the horizontal distance of the circular cylinder, leading to a maximum power coefficient increase of 17.31 percent over a conventional turbine.

Further research is essential to enhance the Savonius wind turbine performance. While previous studies have explored the placement of a circular cylinder either in front of the convex blade or alongside the concave blade, no research has yet combined both configurations. This study aims to evaluate the turbine's performance by incorporating circular cylinders in two distinct arrangements.

## 2. Experimental method

The research was conducted experimentally in a laboratory setting, utilizing two configurations, as illustrated in Figure 1. The Savonius wind turbine featured blades made from polyvinyl chloride (PVC) with the following dimensions: height (H) = 295 mm, blade diameter (D) = 165.2 mm, shaft diameter (e) = 19 mm, and blade thickness (t) = 3 mm. The turbine also included end plates with a diameter (Do) of 320 mm. The circular cylinder used in the study had a height (h) of 490 mm and a diameter (d) of 88.18 mm, resulting in a diameter-to-blade-diameter ratio (d/D) of 0.5. The distance from the center of the circular cylinder next to the concave blade to the turbine center was designated as Y, while the distance from the center of the circular cylinder in front of the convex blade to the center of the convex blade was designated as S. The cylinders were positioned next to the concave blade at a distance ratio of Y/D = 1.42 and in front of the convex blade at S/D = 1.42. Wind speeds (U) were varied at 4, 5, 6, and 7 m/s, corresponding to Reynolds numbers (Re) of 78,000, 97,000, 117,000, and 136,000, respectively, based on the characteristic length (L).

The research scheme is shown in Figure 2. Experiments were conducted in a room relatively unaffected by external wind. An axial fan CKE SF-45H was used as the wind flow source. The airflow from the axial fan was made uniform using a honeycomb placed in front of the fan. The use of honeycomb to ensure uniform airflow has been demonstrated by [23]. The wind speed was regulated by adjusting the voltage on the TDGC2 3KVA voltage regulator.

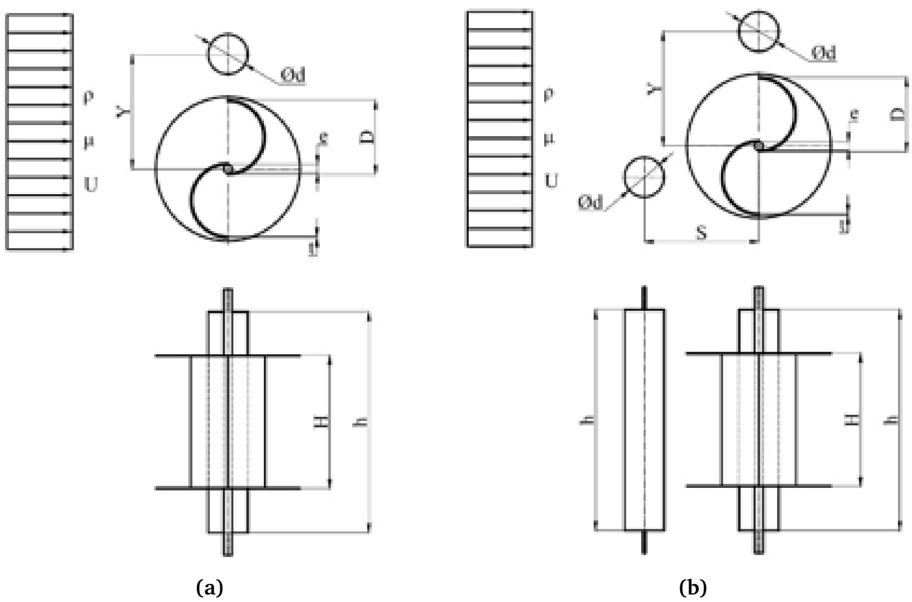


**Figure 1.** (a) First and (b) second configuration

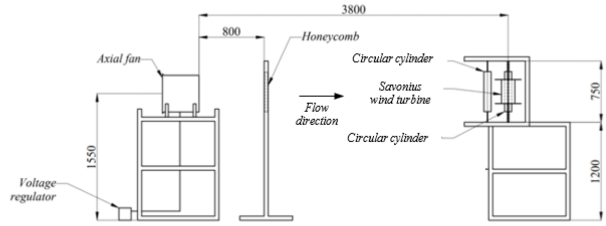


**Figure 2.** Research equipment scheme

An Omega HHF141 anemometer was employed to measure wind speed at a distance of 4.5 times the blade diameter (D) in front of the turbine. A Lutron TQ-8800 torquemeter was utilized to measure static torque. The torquemeter was mounted on the turbine shaft, allowing for static torque measurements at each blade angle position in increments of 10°, from 0° to 180°.

The rotational speed of the turbine was measured using an Omega HHT13 tachometer, which offers an accuracy of ±0.01% and a measurement range of 5 to 200,000 rpm. Dynamic torque was assessed with a brake rope dynamometer, following the methodology established by [24]. As illustrated in Figure 3, the brake rope dynamometer comprised of the following components: (1) Nagata C-5 spring balance, (2) pulley, (3) nylon string, (4) shaft, (5) turbine, and (6) weighing pan. To measure the dynamic torque, weights of 20 g were incrementally added to the brake rope dynamometer until the turbine ceased rotation. The rotational speed of the turbine, spring scale readings, and weights were recorded for each addition and used to determine the dynamic torque. The coefficient of moment ($C_M$) and coefficient of power (CoP) were derived from the dynamic torque and the rotational speed of the turbine, while the coefficient of static torque ($C_{TS}$) was calculated from the turbine's static torque measurements.

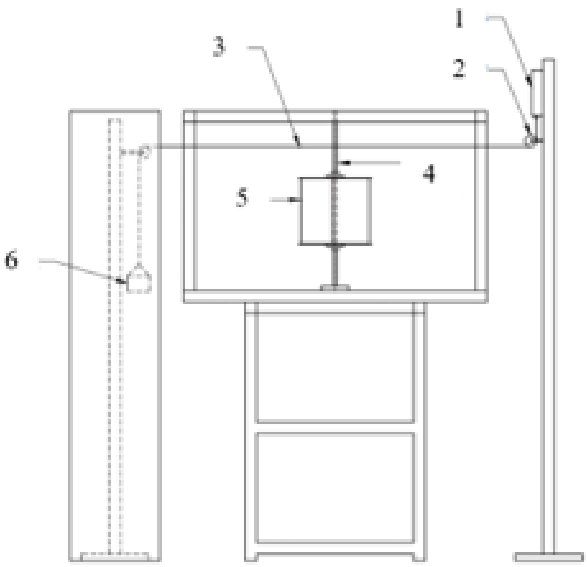


**Figure 3.** Brake rope dynamometer

The turbine characteristic length (L) is defined as

$$L = 2D - 2t - e \tag{1}$$

where D is the blade diameter, t is the blade thickness, and e is the diameter of the shaft. Tip speed ratio ($\lambda$) is defined as the ratio between turbine rotational speed ($\omega$) times the radius of the turbine (R = L/2) to free stream velocity (U). The dynamic torque of the turbine (TD) is defined as

$$T_D = (|s - m|)\, g \times r \tag{2}$$

where s is the spring balance reading, m is mass loading, g is gravitational acceleration, and r is the radius of the pulley. The swept area of the turbine (A) was calculated as the product of the turbine characteristic length (L) and the height of the blade (H). Coefficient of power (CoP), defined as the ratio of the turbine's power output to its input, could be calculated as follows:

$$CoP = \frac{T_D \omega}{\frac{1}{2}\rho A U^3} \tag{3}$$

The coefficient of moment ($C_M$) is the ratio between torque output and theoretical torque output and is defined as

$$C_M = \frac{T_D}{\frac{1}{2}\rho A R U^2} \tag{4}$$

The coefficient of static torque ($C_{TS}$) is the ratio of the static torque produced by the turbine to the theoretical torque of the turbine, computed using the following equation:

$$C_{TS} = \frac{T_S}{\frac{1}{2}\rho A R U^2} \tag{5}$$

where $T_S$ is the static torque

## 3. Results and Discussion

Based on the conducted experiments, values for the coefficient of power, coefficient of moment, and coefficient of static torque of the turbine were obtained. The analysis compared the performance of the conventional turbine, Configuration 1, and Configuration 2 across various wind speeds. Performance results are illustrated through graphs depicting the coefficient of power (CoP) against the tip speed ratio ($\lambda$), the coefficient of moment ($C_M$) against the tip speed ratio ($\lambda$), and the coefficient of static torque ($C_{TS}$) against the blade angle position ($\theta$) for each of the wind speed (U).

### 3.1. Coefficient of Power

Figure 4(a) illustrates the graph of CoP against $\lambda$ for the conventional Savonius turbine, configuration 1, and configuration 2 at U = 4 m/s. The maximum CoP for the conventional turbine is 0.0439 at $\lambda = 0.61$, configuration 1 is 0.0449 at $\lambda = 0.55$, and configuration 2 is 0.0433 at $\lambda = 0.60$. At U = 4 m/s, there is a 2.43% increase in maximum CoP for configuration 1 and a 1.30% decrease in maximum CoP for configuration 2 relative to the conventional turbine.

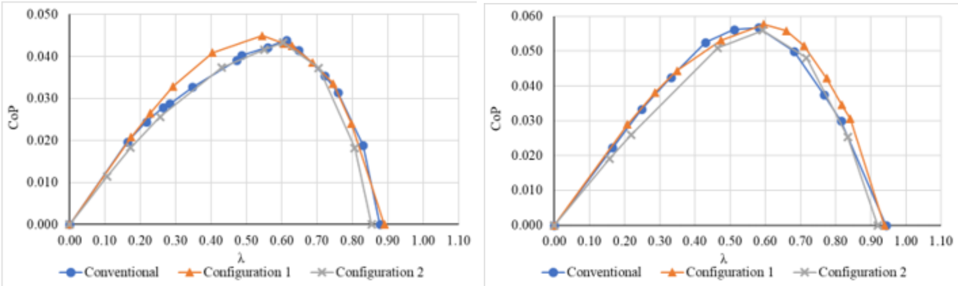


**(a)** **(b)**

**Figure 4.** Graph of CoP against $\lambda$ at U = (a) 4 m/s and (b) 5 m/s

Figure 4(b) illustrates the graph of CoP against $\lambda$ for the conventional Savonius turbine, configuration 1, and configuration 2 at U = 5 m/s. The maximum CoP for the conventional turbine is 0.0567 at $\lambda = 0.58$, configuration 1 is 0.0576 at $\lambda = 0.60$, and configuration 2 is 0.0559 at $\lambda = 0.59$. At U = 5 m/s, there is a 1.60% increase in maximum CoP for configuration 1 and a 1.40% decrease in maximum CoP for configuration 2 relative to the conventional turbine.

Figure 5(a) illustrates the graph of CoP against $\lambda$ for the conventional Savonius turbine, configuration 1, and configuration 2 at U = 6 m/s. The maximum CoP for the conventional turbine is 0.0674 at $\lambda = 0.64$, configuration 1 is 0.0678 at $\lambda = 0.60$, and configuration 2 is 0.0655 at $\lambda = 0.60$. At U = 6 m/s, there is a 0.55% increase in maximum CoP for configuration 1 and a 2.85% decrease in maximum CoP for configuration 2 relative to the conventional turbine.

Figure 5(b) illustrates the graph of CoP against $\lambda$ for the conventional Savonius turbine, configuration 1, and configuration 2 at U = 7 m/s. The maximum CoP for the conventional turbine is 0.0720 at $\lambda = 0.61$, configuration 1 is 0.0723 at $\lambda = 0.60$, and configuration 2 is 0.0688 at $\lambda = 0.60$. At U = 7 m/s, there is a 0.50% increase in maximum CoP for configuration 1 and a 4.35% decrease in maximum CoP for configuration 2 relative to the conventional turbine.

Considering the uncertainty values in the coefficient of power (CoP), the changes in CoP for Configurations 1 and 2 relative to the conventional turbine become statistically insignificant across all wind speed values. The limited performance improvement in Configuration 1 is due to the cylinder next to the concave blade being positioned overly close to the blade, resulting in suboptimal nozzle effects in the space between the cylinder and the concave blade. Although there is a slight increase in velocity within the attached flow region on the concave blade, this only leads to a minor decrease in pressure behind it. Consequently, the pressure difference between the front and back of the concave blade does not increase significantly, preventing a substantial rise in drag force on the concave blade. As a result, the disparity in drag forces between the concave and convex blades does not increase significantly, leading to negligible improvements in torque and power output. This observation aligns with findings from [21, 22], which indicate that a minimal gap does not facilitate optimal performance enhancement.

Similarly, the insignificant performance decrease in Configuration 2 relative to the conventional turbine arises from the cylinder in front of the convex blade positioned overly close to the turbine. The wake generated behind the cylinder does not lower the pressure in front of the convex blade, resulting in no reduction in drag force on that blade. Additionally, the shear layer detached from the cylinder likely influences the already turbulent boundary layer on the convex blade, preventing any delay in the separation point. The wake behind the convex blade does not constrict, meaning there is no drag force reduction on the convex blade. Consequently, there is no increase in the disparity of drag forces between the concave and convex blades, leading to no enhancement in the turbine's torque and power output. This finding is consistent with the results of [25], which demonstrate that positioning a cylinder too close ahead of the convex blade of the turbine does not yield performance improvements.

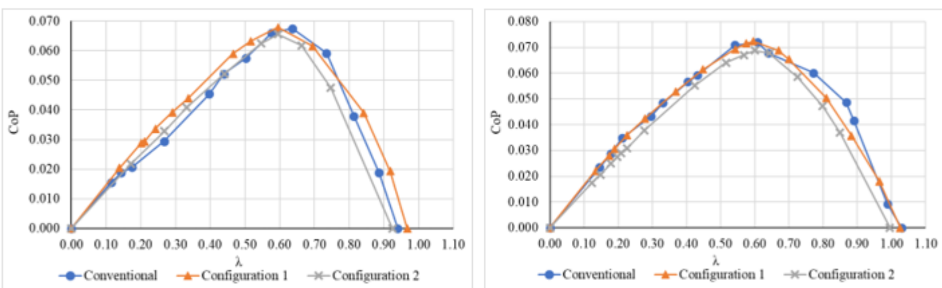


**(a)** **(b)**

**Figure 5.** Graph of CoP against $\lambda$ at U = (a) 6 m/s and (b) 7 m/s

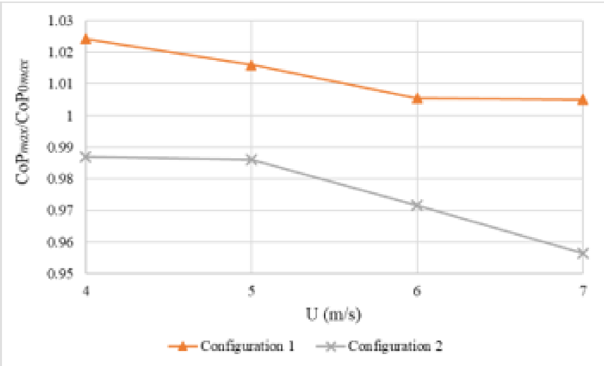


**Figure 6.** Graph of $CoP_{max}/CoP_{0max}$

The graph of $CoP_{max}/CoP_{0max}$ against wind speed (U) for configuration 1 and configuration 2 is shown in Figure 6. and wind speed. $CoP_{max}$ represents the maximum CoP value for a specific configuration, and $CoP_{0max}$ indicates the maximum CoP value of a conventional turbine at a given wind speed. The graph of $CoP_{max}/CoP_{0max}$ against U shows a decreasing trend as U increases. The relative increase in maximum CoP compared to the conventional turbine occurs at U = 4 m/s, with a $CoP_{max}/CoP_{0max}$ value of 1.024 in configuration 1. Thus, the optimal wind speed for the turbine with the addition of a circular cylinder in this study is 4 m/s. However, considering the uncertainty in the maximum CoP for each wind speed, the increase and decrease in CoP relative to the conventional turbine become insignificant.

$CoP_{max}/CoP_{0max}$ value for configuration 1 is higher than that of configuration 2, indicating that configuration 1 is more effective in enhancing turbine performance. In configuration 2, when the turbine blades are at angles between 0° and 30°, the cylinder meant to be positioned in front of the convex blade is located too close to the concave blade. This placement obstructs the flow towards the concave blade, leading to a significant drop in pressure in front of it due to the wake created behind the cylinder. Consequently, the drag force on the concave blade decreases, resulting in lower torque for the turbine at these angles in configuration 2 compared to configuration 1. Additionally, the performance improvement seen in configuration 2 at around 90° blade angle—due to the cylinder's presence in front of the convex blade—is minimal because the cylinder is not optimally positioned. Overall, this indicates that configuration 1 consistently delivers better performance than configuration 2. However, considering the uncertainty in the maximum CoP for each wind speed, the increase and decrease in CoP relative to the conventional turbine become insignificant.

### 3.2. Coefficient of Moment

Figure 7(a) shows the graph of $C_M$ against $\lambda$ for the conventional turbine, configuration 1, and configuration 2 at U = 4 m/s. In the operational range of $\lambda$ for the turbine at U = 4 m/s, which is 0.4 to 0.7, generally, the $C_M$ value for configuration 1 is higher than that of the conventional turbine, while the $C_M$ value for configuration 2 is the same as that of the conventional turbine.

Figure 7(b) shows the graph of $C_M$ against $\lambda$ for the conventional turbine, configuration 1, and configuration 2 at U = 5 m/s. In the operational range of $\lambda$ for the turbine at U = 5 m/s, which is 0.4 to 0.7, generally, the $C_M$ value for configuration 1 is higher than that of the conventional turbine, while the $C_M$ value for configuration 2 is lower than that of the conventional turbine.

Figure 8(a) shows the graph of $C_M$ against $\lambda$ for the conventional turbine, configuration 1, and configuration 2 at U = 6 m/s. In the operational range of $\lambda$ for the turbine at U = 6 m/s, which is 0.4 to 0.8, generally, the $C_M$ value for configuration 1 is higher than that of conventional turbine, while the $C_M$ value for configuration 2 is lower than that of the conventional turbine.

Figure 8(b) shows the graph of $C_M$ against $\lambda$ for the conventional turbine, configuration 1, and configuration 2 at U = 7 m/s. In the operational range of $\lambda$ for the turbine at U = 7 m/s, which is 0.4 to 0.8, generally, the $C_M$ value for configuration 1 is the same as that of the conventional turbine, while the $C_M$ value for configuration 2 is lower than that of the conventional turbine.

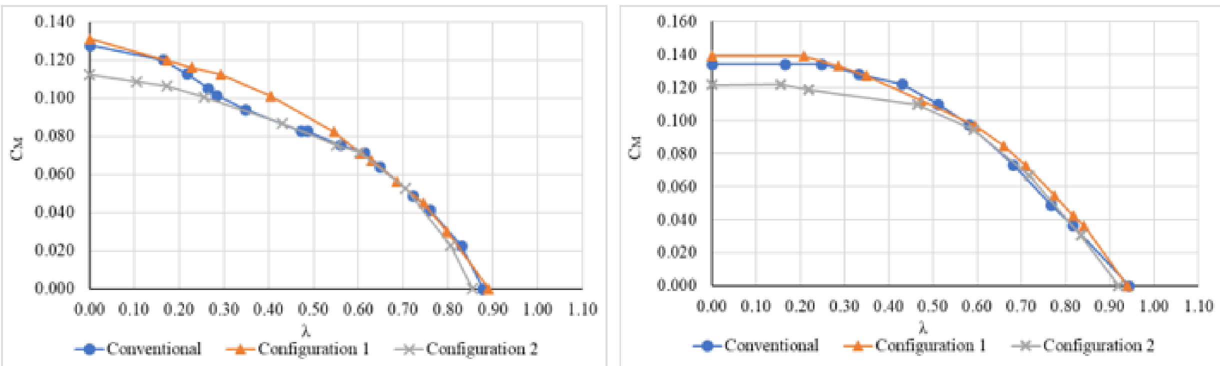


**(a)** **(b)**

**Figure 7.** Graph of $C_M$ against $\lambda$ at U = (a) 4 m/s and (b) 5 m/s

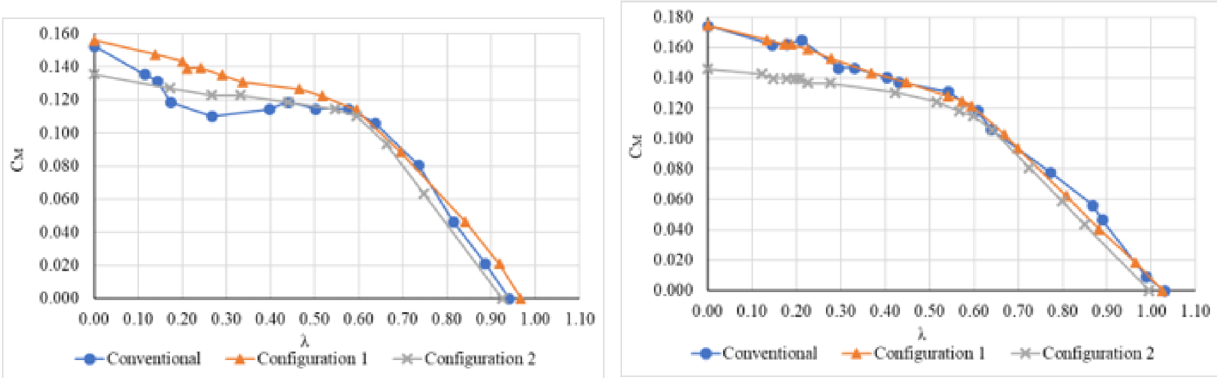


**(a)** **(b)**

**Figure 8.** Graph of $C_M$ against $\lambda$ at U = (a) 6 m/s and (b) 7 m/s

Considering the uncertainty values in $C_M$, the changes in $C_M$ for configurations 1 and 2 relative to the conventional turbine become insignificant for all wind speed values. These results are consistent with the performance analysis derived from CoP. Adding the circular cylinder in configurations 1 and 2 does not yield a significant increase in turbine torque relative to the conventional turbine.

### 3.3. Coefficient of Static Torque

Figure 9(a) illustrates the graph of $C_{TS}$ against $\theta$ for the conventional turbine, configuration 1, and configuration 2 at U = 4 m/s. In configuration 1, for $\theta$ values from 0° to 140° and 170° to 180°, there is an increase in $C_{TS}$ relative to the conventional turbine. In configuration 2, the $C_{TS}$ increases relative to the conventional turbine for $\theta$ values from 30° to 160°.

Figure 9(b) illustrates the graph of $C_{TS}$ against $\theta$ for the conventional turbine, configuration 1, and configuration 2 at U = 5 m/s. In configuration 1, for $\theta$ values from 0° to 140° and 180°, there is an increase in $C_{TS}$ relative to the conventional turbine. In configuration 2, the $C_{TS}$ increases relative to the conventional turbine for $\theta$ values from 30° to 160°.

Figure 10(a) illustrates the graph of $C_{TS}$ against $\theta$ for the conventional turbine, configuration 1, and configuration 2 at U = 6 m/s. In configuration 1, for $\theta$ values from 0° to 140° and 180°, there is an increase in $C_{TS}$ relative to the conventional turbine. In configuration 2, the $C_{TS}$ increases relative to the conventional turbine for $\theta$ values from 30° to 160°.

Figure 10(b) illustrates the graph of $C_{TS}$ against $\theta$ for the conventional turbine, configuration 1, and configuration 2 at U = 7 m/s. In configuration 1, for $\theta$ values from 0° to 140° and 180°, there is an increase in $C_{TS}$ relative to the conventional turbine. In configuration 2, the $C_{TS}$ increases relative to the conventional turbine for $\theta$ values from 30° to 160°.

At wind speeds of U = 4, 5, and 6 m/s, the coefficient of static torque ($C_{TS}$) value at $\theta$ = 120° is negative for the conventional turbine, whereas it is positive for Configuration 1. This indicates that adding the circular cylinder in Configuration 1 enhances the turbine's self-starting capability. Similarly, at wind speeds of U = 4, 5, and 6 m/s, the $C_{TS}$ value between $\theta$ = 120° and 130° remains negative for the conventional turbine but becomes positive for Configuration 2.

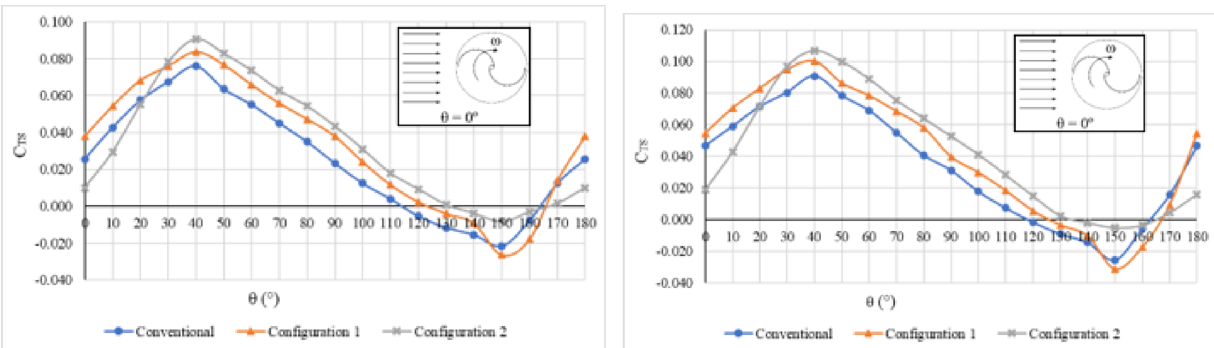


**(a)** **(b)**

**Figure 9.** Graph of $C_{TS}$ against $\theta$ at U = (a) 4 m/s and (b) 5 m/s

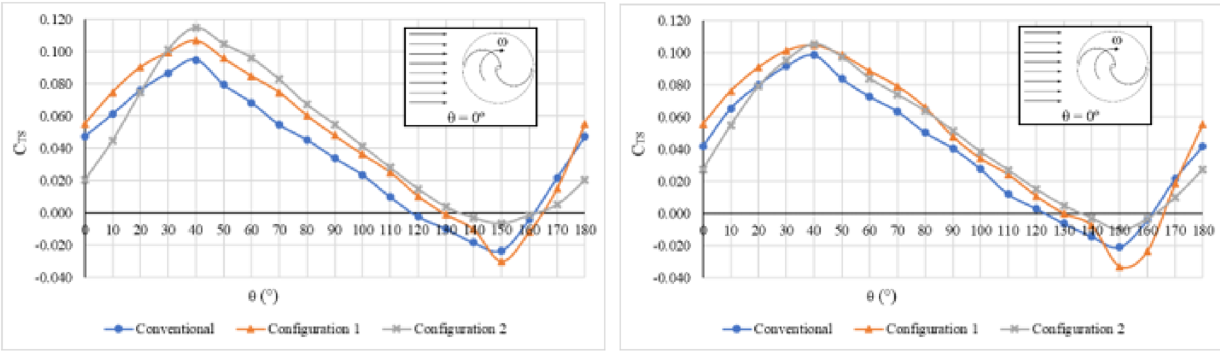


**(a)** **(b)**

**Figure 10.** Graph of $C_{TS}$ against $\theta$ at U = (a) 6 m/s and (b) 7 m/s

Furthermore, at U = 7 m/s, the $C_{TS}$ value at $\theta$ = 130° is negative for the conventional turbine while turning positive for Configuration 2. These results demonstrate that incorporating circular cylinders in Configuration 2 also improves the turbine's ability to self-start.

## 4. Conclusions

The addition of the circular cylinder with a diameter-to-blade-diameter ratio (d/D) of 0.5 next to the concave blade of the Savonius wind turbine at a distance ratio (Y/D) of 1.42 does not yield a significant rise in the coefficient of power or moment. Still, it does enhance the turbine's self-starting capability. Similarly, placing circular cylinders with the same d/D ratio next to the concave blade at Y/D = 1.42 and in front of the convex blade at a distance ratio (S/D) of 1.42 does not enhance the coefficients of power or moment. Still, it also contributes to better self-starting performance; notably, for turbines equipped with the circular cylinder, an increase in wind speed results in a decrease in relative performance compared to the conventional turbine.

This study varied only the wind speed, while keeping the distance between the cylinder and the blade, as well as the stagger angle position of the cylinder, constant. Since these factors likely had a significant impact on turbine performance, it is recommended that future studies investigate the effects of varying the cylinder distance and stagger angle position.

## References


[1] B. P. Statistik, "Hasil sensus penduduk 2020," 2020. URL: `https://www.bps.go.id/pressrelease/2021/01/21/1854/hasil-sensus-penduduk-2020.html` (accessed on 1 April 2024).

[2] B. P. dan Penerapan Teknologi, "Outlook energi indonesia 2021," *Pusat Pengkajian Industri Proses dan Energi*, 2021.

[3] A. Prasetyo, "Studi potensi penerapan dan pengembangan pembangkit listrik tenaga angin di indonesia," *Jurnal Online Mahasiswa (JOM) Bidang Teknik Elektro*, vol. 1, no. 1, pp. 1–12, 2019.

[4] S. Mathew and G. Philip, "Wind turbines: Evolution, basic principles, and classifications," *Comprehensive Renewable Energy, A. Sayigh, Elsevier*, pp. 93–111, 01 2012.

[5] H. Nawir, M. R. Djalal, A. A. Hasri, and A. W. Fauziah, "Modification of the vertical axis with variations in the number of blades of the savonius wind turbine.," *Journal of Advanced Technology & Multidiscipline*, vol. 2, no. 1, pp. 01–08, 2023.

[6] R. Norouztabar, S. S. Mousavi Ajarostaghi, S. S. Mousavi, P. Nejat, S. S. Rahimian Koloor, and M. Eldessouki, "On the performance of a modified triple stack blade savonius wind turbine as a function of geometrical parameters," *Sustainability*, vol. 14, no. 16, p. 9816, 2022.

[7] R. Patel and V. Patel, "Effect of waves on leading edge of modified savonius rotor blades," *Ocean Engineering*, vol. 271, p. 113445, 2023.

[8] A. Prasetyo, M. D. Septiyanto, E. Rovianto, S. Hadi, E. P. Budiana, D. D. D. P. Tjahjana, and I. Yaningsih, "Investigation of blade modifications to enhance savonius water turbine performance through vertical pipe flow," *EVERGREEN Joint Journal of Novel Carbon Resource Sciences and Green Asia Strategy*, vol. 10, no. 01, pp. 564–573, 2023.

[9] J. Ramarajan and S. Jayavel, "Performance improvement in savonius wind turbine by modification of blade shape," *Journal of Applied Fluid Mechanics*, vol. 15, no. 1, pp. 99–107, 2022.

[10] W. Tian, B. Song, J. H. VanZwieten, and P. Pyakurel, "Computational fluid dynamics prediction of a modified savonius wind turbine with novel blade shapes," *Energies*, vol. 8, no. 8, pp. 7915–7929, 2015.

[11] B. D. Altan and M. Atılgan, "An experimental and numerical study on the improvement of the performance of savonius wind rotor," *Energy Conversion and Management*, vol. 49, no. 12, pp. 3425–3432, 2008.

[12] M. Mohamed, G. Janiga, E. Pap, and D. Thévenin, "Optimization of savonius turbines using an obstacle shielding the returning blade," *Renewable Energy*, vol. 35, no. 11, pp. 2618–2626, 2010.

[13] M. Eshagh Nimvari, H. Fatahian, and E. Fatahian, “Performance improvement of a savonius vertical axis wind turbine using a porous deflector,” *Energy Conversion and Management*, vol. 220, p. 113062, 2020.

[14] B. A. Storti, J. J. Dorella, N. D. Roman, I. Peralta, and A. E. Albanesi, “Improving the efficiency of a savonius wind turbine by designing a set of deflector plates with a metamodel-based optimization approach,” *Energy*, vol. 186, p. 115814, 2019.

[15] K. Layeghmand, N. Ghiasi Tabari, and M. Zarkesh, “Improving efficiency of savonius wind turbine by means of an airfoil-shaped deflector,” *Journal of the Brazilian Society of Mechanical Sciences and Engineering*, vol. 42, no. 10, p. 528, 2020.

[16] W. Tian, J. Bian, G. Yang, X. Ni, and Z. Mao, “Influence of a passive upstream deflector on the performance of the savonius wind turbine,” *Energy Reports*, vol. 8, pp. 7488–7499, 2022.

[17] M. Mohamed, G. Janiga, E. Pap, and D. Thévenin, “Optimal blade shape of a modified savonius turbine using an obstacle shielding the returning blade,” *Energy Conversion and Management*, vol. 52, no. 1, pp. 236–242, 2011.

[18] T. Yuwono, G. Sakti, F. Nur Aulia, and A. Chandra Wijaya, “Improving the performance of savonius wind turbine by installation of a circular cylinder upstream of returning turbine blade,” *Alexandria Engineering Journal*, vol. 59, no. 6, pp. 4923–4932, 2020.

[19] G. Sakti and T. Yuwono, “Numerical and experimental investigation of the effect of a circular cylinder as passive control on the savonius wind turbine performance,” *Journal of Southwest Jiaotong University*, vol. 56, pp. 73–93, 12 2021.

[20] P. A. Setiawan, T. Yuwono, and W. A. Widodo, “Effect of a circular cylinder in front of concave blade on the savonius water turbine by using transient simulation,” *International Journal of Mechanical and Mechatronics*, vol. 19, no. 01, pp. 151–159, 2019.

[21] P. Setiawan, T. Yuwono, and W. Widodo, “Flow analysis of a circular cylinder on the savonius hydrokinetic turbine performance placed the side of advancing blade,” *International Journal of Mechanical and Mechatronics Engineering*, vol. 19, no. 06, pp. 41–48, 2019.

[22] P. A. Setiawan, T. Yuwono, W. A. Widodo, E. Julianto, and M. Santoso, “Numerical study of a circular cylinder effect on the vertical axis savonius water turbine performance at the side of the advancing blade with horizontal distance variations,” *International Journal of Renewable Energy Research*, vol. 9, no. 2, pp. 978–985, 2019.

[23] N. P. Putri, T. Yuwono, J. Rustam, P. Purwanto, and G. Bangga, “Experimental studies on the effect of obstacle upstream of a savonius wind turbine,” *SN Applied Sciences*, vol. 1, p. 1216, 2019.

[24] N. Mahmoud, A. El-Haroun, E. Wahba, and M. Nasef, “An experimental study on improvement of savonius rotor performance,” *Alexandria Engineering Journal*, vol. 51, no. 1, pp. 19–25, 2012.

[25] T. Y. Yuwono, R. A. Bagas, P. Suksmatatya, M. M. Festy, L. Elza, N. A. Vega, J. Dionisius, L. B. Michael, and S. Afiyah, “Enhancing savonius turbine self-starting capability by installing a circular cylinder in front of returning turbine blade,” *JMES The International Journal of Mechanical Engineering and Sciences*, vol. 5, no. 1, pp. 16–23, 2021.